

# FULL-FIELD MAMMOGRAM ANALYSIS BASED ON THE IDENTIFICATION OF NORMAL REGIONS

Yajie Sun †, Charles Babbs ‡, and Edward J. Delp †

†Video and Image Processing Laboratory  
School of Electrical and Computer Engineering  
Purdue University  
West Lafayette, IN 47907-1285

‡Department of Basic Medical Sciences  
School of Veterinary Medicine  
Purdue University  
West Lafayette, IN 47907-1246

## ABSTRACT

We present a new method for full-field mammogram analysis. A mammogram is analyzed region by region and is classified as normal or abnormal. We present methods for extracting features that can be used to distinguish normal and abnormal regions of a mammogram. We describe our classifier technique that uses a unique re-classification method to boost the classification performance. We have tested this technique on a set of ground-truth full-field mammograms.

## 1. INTRODUCTION

Breast cancer is the leading cause of cancer-related death among women aged 15-54. The earlier breast cancer is detected, the higher is the chance of survival. Screening mammography is the only method currently available for the reliable detection of early and potentially curable breast cancer.

Several studies have shown retrospectively that 20% to 40% of breast cancers fail to be detected at screening [1]. A computer-aided detection (CAD) system has been developed as a second reader. The performance of the radiologists can be increased 5-15% by providing the radiologists with results from a CAD system as a “second opinion” [2]. However, the majority of mammograms are normal. Among the false positive readings of normal mammograms, only 15%-34% actually show malignancy at histological examination [3]. An accurate computer-aided system to identify normal mammograms would reduce radiologists’ workload, allow them to focus more on suspicious cases and to improve screening performance.

In this paper, we propose a new method of full-field mammogram analysis based on the identification of normal regions. First, a classifier for identifying normal regions, is trained from a set of features extracted from normal and

ground-truth cancerous regions extracted from the DDSM (Digital Database for Screening Mammography) database [4]. Using an overlapped block technique, this classifier is used to analyze full-field mammograms. This approach is independent of the type of abnormality, and may complement computer-aided detection.

## 2. FULL-FIELD MAMMOGRAM ANALYSIS

The following sections discuss each step of our full-field analysis technique and is outlined in Figure 1.

### 2.1. Mammogram Database

All of the mammograms used in this study are obtained from the Digital Database for Screening Mammography (DDSM) [4]. Each mammogram has been “normalized” to optical density and linearly mapped to an 8-bit gray level image.

We use the breast-background separation method described in [5] to segment out the breast area. The segmented image is ready for full-field analysis.

### 2.2. Enhancement Based on $h_{int}$ Representation

A standardized mammogram representation can be based on modelling of the X-ray physics of the image formation process. We used the techniques described in [6] that models the complete imaging process and compensates the degrading factors, such as scattering. The resulting image, known as the  $h_{int}$  representation, records the height of non-fatty tissue in the breast for each pixel in the image. This measurement is intrinsic to the breast.

In our experiment, we used a simplified transform based on a mono-energetic  $h_{int}$  and an enhancement step to remove the background. We call the processed image  $I_E$ . All of features will be extracted from  $I_E$ .

---

Address all correspondence to Dr. E. J. Delp, ace@ecn.purdue.edu. This work was supported by a grant from CADx Systems Inc.

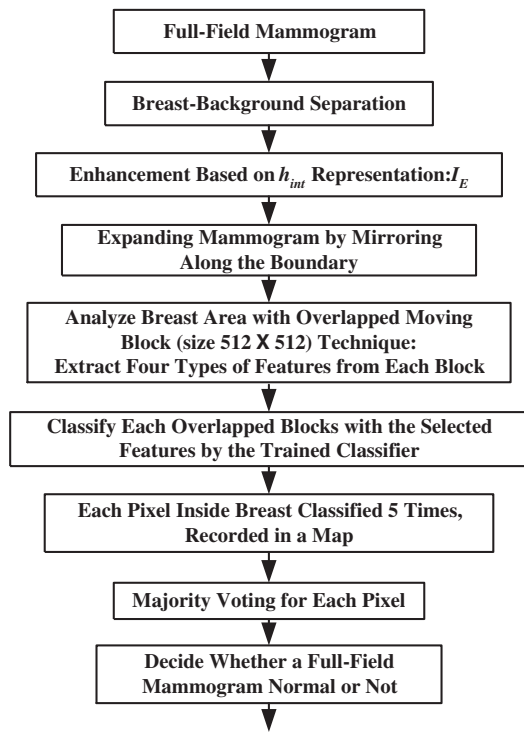


Fig. 1. Full-Field Mammogram Analysis

### 2.3. Regional Feature Extraction

Each full-field mammogram is analyzed by overlapped moving blocks. The region covered by each block is  $512 \times 512$  pixels. There are four types of features extracted from each region: *curvilinear features*, *texture features*, *Gabor features*, and *multi-resolution features*.

*Curvilinear features*: Though normal breast tissue may have very different appearance, unequivocally normal breast areas are characterized by curvilinear markings. These curvilinear structures are the ductal structures of the breast tissue. We used a line detection algorithm we previously developed [7] to extract the curvilinear structures in each region. The algorithm is robust to noise and is capable of extracting quasi-linear curves of different widths and angles. A set of features was extracted from the detected curvilinear structures to characterize the region. There were total 18 curvilinear features extracted for each region, capturing the statistical nature of the line pixels.

*Texture features*: Texture information is characterized by the spatial arrangement of the pixel intensities. This can be specified by a 2D spatial dependence matrix known as the Gray Level Co-occurrence Matrix (GLCM) [8]. GLCM is one of the best known texture analysis methods. We extracted 16 features from the GLCM, as defined in [8] and additional cluster features as defined in [9].

*Gabor features*: Gabor filters has been used for texture analysis for many years [10]. The advantage of Gabor filters is that they provide simultaneous localization in both the spatial and frequency domains. In the study, the highest and lowest frequencies of the Gabor filter-bank were chosen to suit our analysis. We chose 4 orientations and 4 scales for the Gabor filter-bank. We obtained the mean and standard deviation of the energy of each Gabor filtered image. Hence, there were 32 Gabor features extracted from each region.

*Multi-resolution features*: The last type of features were obtained from a nonlinear wavelet decomposition. A special nonlinear wavelet transform, the Quincunx Wavelet transform [11], was used in our study. Only the first four even-level wavelet decomposition images were retained for feature extraction. Five features were extracted from each decomposition for a total of 20 features.

The above four types of features combined to form a 86-feature vector associated with each  $512 \times 512$  region. These will be used to train a cascading classifier.

### 2.4. A Cascading Classifier For Identifying Normal Regions

A cascading classifier, shown in Figure 2, was trained using the  $512 \times 512$  regions. These regions were manually extracted from screening mammograms different than the mammograms used for testing. All of normal regions were extracted from normal mammograms and cancerous regions were extracted from cancer cases with the cancer in the center of the region. A total of 460 training regions were used, which consisted of 296 normal and 164 cancer regions. The training procedure was performed only once. After the training, the classifier is used to analyze each full-field mammogram region by region.

The two-stage cascading classification system (in Figure 2) is a special case of the stacked generalization [12] due to its layered structure. The first stage should correctly classify most of the abnormal regions while separating out as many of the normal regions as possible. A binary decision tree classifier described in [13] was used as the first stage classifier because it is one of the most powerful classification tools. Misclassification costs could be specified to retain almost all training cancerous regions.

The decision tree classifier was based on a hierarchy of multiple decision variables (features), which made it difficult to evaluate the performance using a Receiver Operation Curve (ROC). Therefore, in addition to improving the classification performance, a second-stage classifier was used. Only those regions classified as “abnormal” by the decision tree classifier were classified by the second-stage. In this study, the second-stage classifier was a linear classifier with adaptive floating search feature selection [14]. This two-stage cascading classifier system has the classification

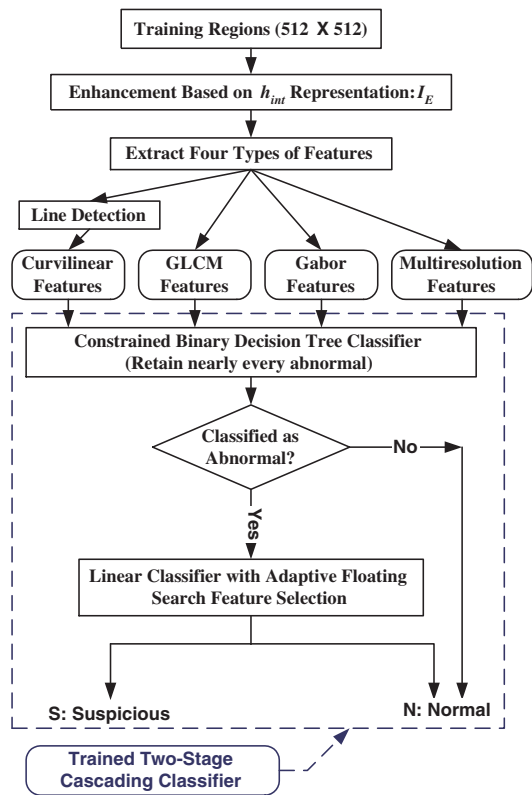


Fig. 2. A cascading classifier for identifying normal regions

power of a decision tree and the simplicity of the ROC analysis of a linear classifier. Our experiments showed that it performed better than a decision tree or a linear classifier.

### 2.5. Full-field Analysis Using Overlapped Regions

The cascading classifier was used to analyze a full-field mammogram using an overlapped, moving block technique. The moving block size is  $512 \times 512$ . First, each mammogram was expanded by mirroring 128 pixels along the boundary to reduce the edge effects. The breast area is analyzed by 5 overlapped blocks. The block is centered on a pixel and then is moved by 128 pixels up, down, right, and left. Using the two-stage cascading classifier on each block, the classification result (normal or abnormal) of each block is obtained, therefore each subregion is classified 5 times. A majority voting scheme is used to determine the final classification (Figure 1). Finally, a full-field mammogram is classified as a cancer image if one or more subregions are abnormal, otherwise, the mammogram is classified as a normal.

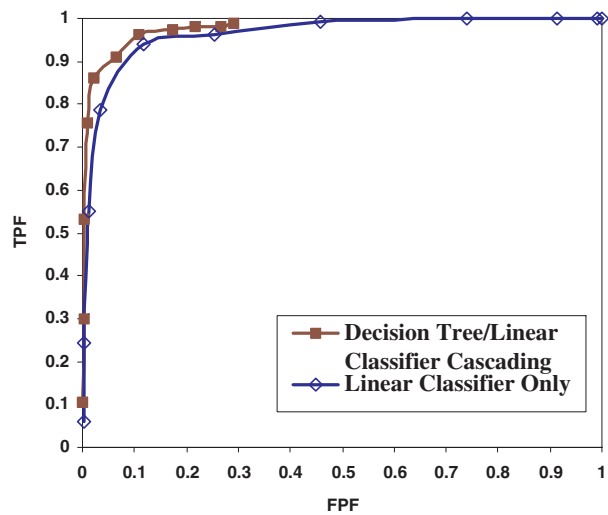


Fig. 3. The overall performance of our two-stage cascading regional classifier ( $A_z = 0.98$ ), comparison with a linear classifier ( $A_z = 0.96$ )

## 3. RESULTS

Our two-stage cascading classifier was trained from an independent training set of 164 ground-truth cancerous regions and 296 normal regions. Among the 164 ground-truth cancerous regions, 53 were masses, 56 were spiculations and 55 were calcifications. The first-stage decision tree classifier was constrained to retain nearly every cancerous region. This resulted in a True Positive Fraction (TPF) of 0.99 at a False Positive Fraction (FPF) of 0.29. The regions (including 162 true positives and 86 false positives) classified as “abnormal” were then refined by the second-stage linear classifier. Our two-stage classifier system had an overall performance,  $A_z = 0.98$ , where  $A_z$  is the area under the ROC. Figure 3 shows the comparison with a linear classifier, with  $A_z$  of 0.96.

Table 1. Normal Classification on Cancer Mammograms

Number of Correct Classifications of Different Cancers		
Calcifications	Mammograms Tested	25
	Classified As Abnormal	17
Masses	Mammograms Tested	22
	Classified As Abnormal	20
Spiculations	Mammograms Tested	22
	Classified As Abnormal	21

The classifier was then used to analyze full-field mammograms. We tested 71 cancer mammograms and 76 normal mammograms. Among the 71 cancer mammograms,

25 were calcification images, 22 were mass images and 24 were spiculation images. Table 1 shows the performance on full-field cancer mammograms. The true positive rate is 0.82. Most of misclassified cancer images are calcifications. The region of analysis might be too large for small clusters of calcifications. Excluding calcifications, we obtain nearly 90% correct classification on mass and spiculation images. We believe the reason for misclassification is due to the subtlety of the breast cancers. 57 normal mammograms are classified correctly, i.e. the true negative rate is 0.75. Most of misclassification is due to high breast density of these normal mammograms.

#### 4. CONCLUSIONS

A new full-field mammogram analysis method was presented. Our initial results are encouraging. We intend to continue this study using a larger database of both scanned images and images obtained from a digital mammography system.

#### 5. REFERENCES

- [1] C. Beam, P. Layde, and D. Sullivan, "Variability in the interpretation of screening mammograms by us radiologists, findings from a national sample," *Archives of Internal Medicine*, vol. 156, pp. 209–213, 1996.
- [2] E.L. Thurfjell, K.A. Lernevall, and A.S. Taube, "Benefit of independent double reading in a population-based mammography screening program," *Radiology*, vol. 191, pp. 241–244, 1994.
- [3] J.Y. Lo, J.A. Baker, P.J. Kornguth, J.D. Iglehart, and C.E. Floyd, "Predicting breast cancer invasion with artificial neural networks on the basis of mammographic features," *Radiology*, vol. 203, pp. 159–163, 1997.
- [4] M. Heath, K.W. Bowyer, D. Kopans, R. Moore, and Jr. P. Kegelmeyer, "The digital database for screening mammography," *Proceedings of the 5th International Workshop on Digital Mammography*, pp. 212–218, June 11-14 2000.
- [5] T. Ojala, J. Näppi, and O. Nevalainen, "Accurate segmentation of the breast region from digitized mammograms," *Computerized Medical Imaging and Graphics*, vol. 25, pp. 47–59, 2001.
- [6] Ralph Highnam and Michael Brady, *Mammographic Image Analysis*, Kluwer Academic Publishers, Dordrecht, 1999.
- [7] S. Liu, *The Analysis of Digital Mammograms: Spiculated Tumor Detection and Normal Mammogram Characterization*, Ph.D. Thesis, School of Electrical and Computer Engineering, Purdue University, May 1999.
- [8] R.M. Haralick, K. Shanmugam, and I. Dinstein, "Textural features for image classification," *IEEE Trans. On Systems, Man, and Cybernetics*, vol. SMC-3, no. 6, pp. 610–621, November 1973.
- [9] R.W. Connors, M.M. Trivedi, and C.A. Harlow, "Segmentation of a high-resolution urban scene using texture operators," *Computer Vision, Graphics and Image Processing*, vol. 25, no. 3, pp. 273–310, 1984.
- [10] B.S. Manjunath and W. Y. Ma, "Texture features for browsing and retrieval of image data," *IEEE Trans. On Pattern Analysis and Machine Intelligence*, vol. 18, no. 8, pp. 837–842, August 1996.
- [11] J. Kovačević and M. Vetterli, "Nonseparable multidimensional perfect reconstruction filter banks and wavelet bases for  $R_n$ ," *IEEE Transactions on Information Theory*, vol. 38, no. 2, pp. 535–555, March 1992.
- [12] D. Wolpert, "Stacked generalization," *Neural Networks*, vol. 5, 1992.
- [13] S.B. Gelfand, C.S. Ravishankar, and E.J. Delp, "An iterative growing and pruning algorithm for classification tree design," *IEEE Transaction on Pattern Analysis Machine Intelligence*, vol. 13, pp. 163–174, 1991.
- [14] P. Somol, P. Pudil, J. Novovicova, and P. Paclik, "Adaptive floating search methods in feature selection," *Pattern Recognition Letters*, vol. 20, pp. 1157–1163, 1999.